Article

The Oxidation-State Dependent Structural Conformation and Supramolecular Function of a Redox-Active [2]Rotaxane in Solution

Kirill Nikitin, and Donald Fitzmaurice

J. Am. Chem. Soc., **2005**, 127 (22), 8067-8076• DOI: 10.1021/ja050694h • Publication Date (Web): 13 May 2005

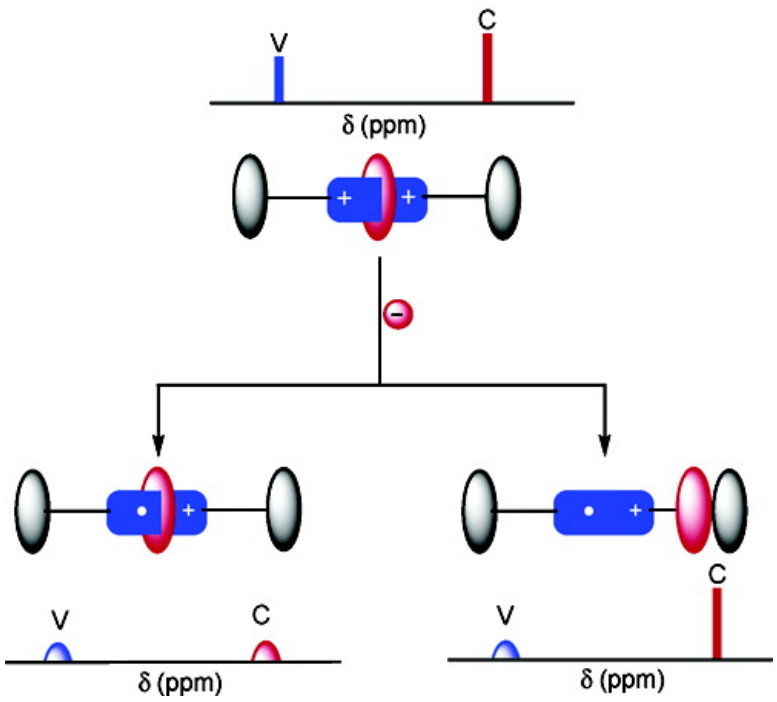

More About This Article

Additional resources and features associated with this article are available within the HTML version:

- Supporting Information
- Links to the 7 articles that cite this article, as of the time of this article download
- Access to high resolution figures
- Links to articles and content related to this article
- Copyright permission to reproduce figures and/or text from this article

View the Full Text HTML

J|A|C|S
ARTICLES
Published on Web 05/13/2005

The Oxidation-State Dependent Structural Conformation and Supramolecular Function of a Redox-Active [2]Rotaxane in Solution

Kirill Nikitin and Donald Fitzmaurice*

Contribution from the Department of Chemistry, University College Dublin, Belfield, Dublin 4, Ireland

Received February 2, 2005; E-mail: donald.fitzmaurice@ucd.ie.

Abstract: A new NMR technique, namely paramagnetic suppression spectroscopy (PASSY), has been used to study the oxidation-state dependent structural conformation and supramolecular function of redox-active rotaxanes and catenanes in solution and at the surfaces of nanoparticles. Specifically, this technique has been used to study the structural conformation and supramolecular function in solution of a redox-active [2]rotaxane and the corresponding radical cation formed by a one-electron reduction. The findings of this and related studies provide important insights into the design of nanoscale devices based on rotaxanes and catenanes.

Introduction

The bottom-up assembly of functional nanoscale architectures in solution and at surfaces is a goal shared by researchers in many fields.[1] Expected benefits include greater control over material properties and innovative technologies that address unmet needs.[2] One approach envisaged is the self-assembly of functional nanoscale architectures from molecular and condensed phase components.[3]

In considering what molecular and condensed phase components might be suitable,[4−6] one is attracted to the growing number of supermolecules and nanoparticles possessing well-defined functions and properties.[7,8] It is in this context that we and others have synthesized supermolecules incorporating linkers that can be used to adsorb supermolecules at the surface of nanoparticles.[9−14]

Specifically we have synthesized rotaxanes, incorporating tripodal linkers, that can be used to adsorb these supermolecules at the surface of both metal and semiconductor nanoparticles. Our interest in rotaxanes is a consequence of the development of simple and reliable synthetic methods, which can be used to prepare increasingly complex rotaxanes in good yields,[9,15] and their potential use as components in nanoscale devices that can be used to process information and effect motion.

More specifically we have synthesized the hetero[2]rotaxane shown in Scheme 1.[9,11] The phosphonate moieties of the linker strongly bind the viologen-based axle of the [2]rotaxane to the surface of the titanium dioxide nanoparticle. Their tripodal arrangement orients the axle normal to and displaces it from the surface of the nanoparticle. The inherent bulkiness of the tripodal linker reduces the possibility of unwanted lateral interactions.

The structure and function of the hetero[2]rotaxane shown in Scheme 1 have been studied in detail by ^{1}H NMR spectroscopy, optical absorption spectroscopy, and cyclic voltammetry.[11] A key finding is that the most probable location of the crown depends on the oxidation state of the two viologens in the axle and on the structural conformation of the axle linked to the surface of the titanium dioxide nanoparticle.

Initially, the electron-rich crown ether (**C**) spends most of the time in the vicinity of the more electron-poor viologen adjacent to the tripodal linker ($\mathbf{V_1}$) and is said to be localized there. On the basis of previous reports,[16] it was expected that a single one-electron reduction of $\mathbf{V_1}$ would result in **C** shuttling to and being localized at the initially less electron-poor viologen

(1) (a) Philp, D.; Stoddart, J. F. *Angew. Chem., Int. Ed. Engl.* **1996**, *35*, 1154−1196. (b) Flood, A.; Ramirez, R.; Deng, W.-Q.; Muller, R.; Goddard, W.; Stoddart, J. F. *Aust. J. Chem.* **2004**, *57*, 301−322.
(2) Bows, W. *Investors Chron.* **2002**, *139*, 30−32.
(3) (a) Whitesides, G. M.; Mathias, J. P.; Seto, C. T. *Science* **1991**, *254*, 1312−1319. (b) Kalsani, V.; Ammon, H.; Jackel, F.; Rabe J. P.; Schmittel, M. *Chem. Eur. J.* **2004**, *10*, 5481−5492.
(4) Service, R. F. *Science* **1997**, *277*, 1036−1037.
(5) Mann, S.; Shenton, W.; Li. M.; Connolly, S.; Fitzmaurice, D. *Adv. Mater.* **2000**, *12*, 147−150.
(6) Niemeyer, C. *Angew. Chem., Int. Ed.* **2001**, *40*, 4128−4158.
(7) Lehn, J.-M. *Supramolecular Chemistry, Concepts and Perspectives* VCH: Weinheim, **1995**.
(8) (a) Alivisatos, A. P. *Science* **1996**, *271*, 933−937. (b) Mendes, P. M.; Chen, Y.; Palmer, R. E.; Nikitin, K.; Fitzmaurice, D.; Preece, J. A. *J. Phys.: Condens. Matter* **2003**, *14*, S3047−3063.
(9) Nikitin, K.; Long, B.; Fitzmaurice, D. *J. Chem. Soc., Chem. Commun.* **2003**, 282−283.
(10) Long, B.; Nikitin, K.; Fitzmaurice, D. *J. Am. Chem. Soc.* **2003**, *125*, 5152−5160.
(11) Long, B.; Nikitin, K.; Fitzmaurice, D. *J. Am. Chem. Soc.* **2003**, *125*, 15490−15498.
(12) Galoppini, E.; Guo, W. *J. Am. Chem. Soc.* **2001**, *123*, 4342−4343.
(13) Galoppini, E.; Guo, W.; Zhang, W.; Hoetz, P. G.; Qu, P.; Meyer G. J. *J. Am. Chem. Soc.* **2002**, *124*, 7801−7811.
(14) Hoertz, P.; Carlisle, R.; Meyer, G. J.; Wang, D.; Piotrowiak, P.; Galoppini, E. *Nano Lett.* **2003**, *3*, 325−330.
(15) Katz, E.; Lioubashevsky, O.; Willner, I. *J. Am. Chem. Soc.* **2004**, *126*, 15520−15532.
(16) Ashton, P. R.; Ballardini, R.; Balzani, V.; Credi, A.; Ruprecht-Dress, K.; Ishow, E.; Kleverlaan, C.; Kocian, O.; Preece, J.; Spencer, N.; Stoddart, J. F.; Venturi, M.; Wenger, S. *Chem. Eur. J.* **2000**, *6*, 3558−3574.

Scheme 1. Hetero[2]rotaxane

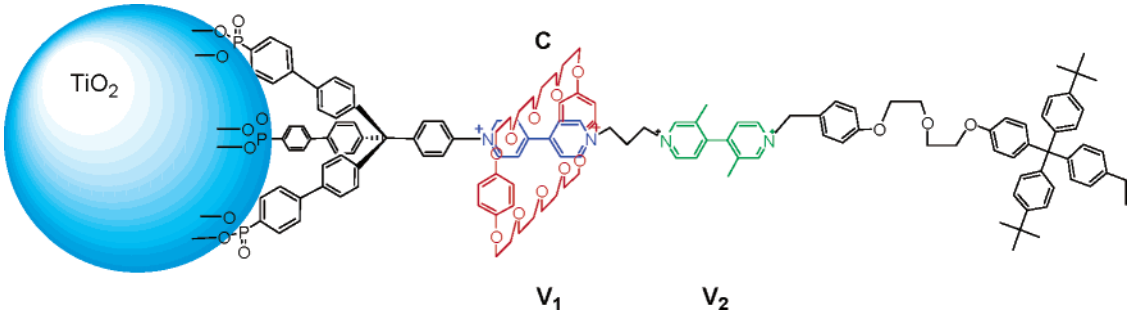

adjacent to the bulky stopper ($\mathbf{V_2}$). It was found, however, that a one-electron reduction of $\mathbf{V_1}$ did not result in **C** being localized at $\mathbf{V_2}$. This was observed only after a second one-electron reduction of $\mathbf{V_1}$. Having localized **C** at $\mathbf{V_2}$, it was expected that two successive one-electron reductions of $\mathbf{V_2}$ would result in **C** being fully delocalized and free to move along the entire length of the axle. It appears, however, that the second of these two one-electron reductions is accompanied by a significant change in the structural conformation of the axle. As a consequence, it is most likely that the translational motion of **C** is restricted. On this basis it was concluded that the electromechanical properties of the hetero[2]rotaxane in Scheme 1 depend not only on its oxidation state of the axle but also on its structural conformation.

Since we first reported these findings, a number of groups have reported related observations, also suggesting that the oxidation state and structural conformation of rotaxanes and heterorotaxanes are related.[17−20] It is clear that a deeper understanding of this relationship will be essential to fully exploit the potential technological applications of these and related supermolecules.[15,21]

It is in this context that we have developed a new NMR technique, namely paramagnetic suppression spectroscopy (PASSY), that can be used to examine the structural conformation of redox-active rotaxanes and catenanes in different oxidation states in solution and at the surfaces of nanoparticles. Here we describe the use of PASSY to study the structural conformation in solution of a redox-active [2]rotaxane and the corresponding radical cation formed by a one-electron reduction. The findings of this study provide important insights into the relationship between the oxidation-state dependent structural conformation of the redox-active [2]rotaxane and its associated supramolecular function.

Results and Discussion

PASSY Technique. NMR is one of the most powerful tools available for molecular structure determination in solution and, increasingly, at the surfaces of nanoparticles. One NMR technique, namely the measurement of spin−lattice relaxation rates,[22] has been demonstrated to be very effective and is routinely used for protons.

The above technique involves irradiating a proton at its resonant frequency. This results in a non-Boltzman-like distribution of protons between the two available magnetic energy levels. Following irradiation, the equilibrium distribution of protons between these energy levels is re-established by energy transfer to the surrounding environment. The first-order rate constant for this spin−lattice relaxation process is R_1. The inverse of this rate constant is the spin−lattice relaxation time T_1, that is the time required for 63% of the excess population of protons in the upper magnetic energy level to return to the lower energy level.

The principal mechanism by which the energy of an excited proton is transferred to the surroundings is dipole−dipole coupling.[23] This mechanism requires the relative motion of two protons that are close to each other at a frequency corresponding to the energy of separation between the two magnetic energy levels. The corresponding rate constant R_1^{DD} is given by eq 1, where γ_{P1} and γ_{P2} are the magnetic dipole moments of the two protons, r is the distance separating the two protons, and τ_c is the correlation time for rotational motion of the molecule. β is a constant.

$$R_1^{DD} = \frac{1}{T_1} = \beta \gamma_{P_1}{}^2 \gamma_{P_2}{}^2 r^{-6} \tau_c \qquad (1)$$

In paramagnetic molecules, the coupling of the magnetic dipole of a proton and the magnetic dipole of the unpaired electron leads to very significantly increased rates of spin−lattice relaxation.[24] This effect, termed paramagnetic relaxation enhancement (PRE), results in broadening, often to the extent of disappearance, of the resonances assigned to protons that are close to the unpaired electron.

More quantitatively, the paramagnetic contribution to the measured rate of relaxation R_1^e is given by eq 2, where γ_P and γ_e are the proton and electron magnetic dipole moments, r is the nucleus-electron separation, and τ_e is the electron correlation time. β' is a constant.

$$R_1 = \frac{1}{T_1^e} \beta' \gamma_P{}^2 \gamma_e{}^2 r^{-6} \tau_e \qquad (2)$$

In practice, the rate constant for relaxation is the sum of the rate constants for dipole−dipole and paramagnetic relaxation and is given by eq 3.

(17) Kim, K.; Jeon, W.; Kang, J.-K.; Lee, J.; Jon, S.; Kim, T.; Kim, K. *Angew. Chem., Int. Ed.* **2003**, *42*, 2293−2296.
(18) Azehara, H.; Mizutani, W.; Suzuki, Y.; Ishida, T.; Nagawa, Y.; Tokumoto, H.; Hiratani, K. *Langmuir* **2003**, *19*, 2115−2123.
(19) Hernandez, R.; Tseng, H.-R. Wong, J.; Stoddart, J. F.; Zink, J. *J. Am. Chem. Soc.* **2004**, *126*, 3370−3371.
(20) Katz, E.; Sheeney-Haj-Ichia, L.; Willner, I. *Angew. Chem., Int. Ed.* **2004**, *43*, 3292−3300.
(21) Collier, C.; Wong, E.; Belohradsky, M.; Raymo, F.; Stoddart, J. F.; Kuekes, P.; Williams, R.; Heath, J. *Science* **1999**, *285*, 391−394.
(22) Sohar, P. *Nuclear Magnetic Resonance Spectroscopy*; CRC Press: New York, 1983; Vol. I.
(23) Hubbard, P. *Phys. Rev.* **1963**, *131*, 1155−1165.
(24) Sharp, R.; Lohr, L.; Miller, R. *Prog. Nucl. Magn. Reson. Spec.* **2002**, *38*, 115−158.

$$R_1 = R_1^{DD} + R_1^{e}$$
$$\frac{1}{T_1} = \frac{1}{T_1^{DD}} + \frac{1}{T_1^{e}} \quad (3)$$

As discussed in the Introduction, rotaxanes are attracting the attention of an increasing number of research groups. Many of these rotaxanes consist of either an axle or a ring which, when reduced or oxidized, causes a change in the equilibrium position of the components of the rotaxane. Often the oxidation or reduction of such rotaxanes results in the formation of a paramagnetic species. The NMR spectra of paramagnetic molecules contain a great deal of information, which can be used to elucidate the structural conformation changes that accompany oxidation or reduction. To illustrate this we consider the nominal [2]rotaxane shown in Scheme 2.

This nominal [2]rotaxane consists of a redox-active axle, specifically a viologen dication **V**, and a redox-inactive ring, specifically a crown ether **C**. Initially, the electron-rich **C** is localized at the electron-poor **V**. If **V** is reduced to form the corresponding radical cation, two outcomes can be envisaged. First, **C** continues to be localized at **V**. For this outcome, it is expected that the resonances assigned to both **C** and **V** will show significant broadening or even disappear as a result of PRE. Second, **C** is no longer localized at **V**. For this outcome, the resonances assigned to **V** will broaden or even disappear as a result of PRE, while those assigned to **C** would be expected to show only slight broadening. A further outcome may be envisaged if the redox-active axle undergoes a structural conformational change following reduction or oxidation. For this outcome, it is expected that the resonances assigned to protons at either end of the axle will experience a change in the magnitude of the PRE. These changes can be used to elucidate these structural conformational changes.

This approach was applied to the model axles, the model [2]pseudorotaxane and the model [2]rotaxane, shown in Schemes 3−5 (see below). The initial objective was to understand the relationship between the oxidation states of these compounds and their structural conformations in solution. The ultimate objective was to draw conclusions about the relationship between the oxidation-state dependent structural conformation of the above redox-active [2]pseudorotaxane and [2]rotaxane and its associated supramolecular function.

Design and Synthesis of Model Compounds. The model axles **1**·2PF_6−**3**·2PF_6 belong to a class of heterocyclic 1,1′-disubstituted 4,4′-bipyridinium compounds called viologens and are shown in Scheme 3. These axles all reversibly thread the crown ether **5** to form [2]pseudorotaxanes. For example, the axle **1**·2PF_6 reversibly threads the crown ether **5** to form the [2]pseudorotaxane **1**·**5**·2PF_6 as shown in Scheme 4. Axles incorporating bulky stopper groups, when interlocked with the crown ether **5**, form [2]rotaxanes. For example, the axle **4**·2PF_6 when interlocked with the crown ether **5** forms the [2]rotaxane **4**·**5**·2PF_6.

Each of the above axles **1**−**4**, whether free in solution or incorporated into the [2]pseudorotaxane **1**·**5**·2PF_6 or [2]rotaxane **4**·**5**·2PF_6, will accept an electron to form the corresponding radical cation. The effect of the unpaired electron on the proton NMR spectra and, more specifically, on the proton relaxation times was studied in detail.

Scheme 2. Illustration of PASSY Technique

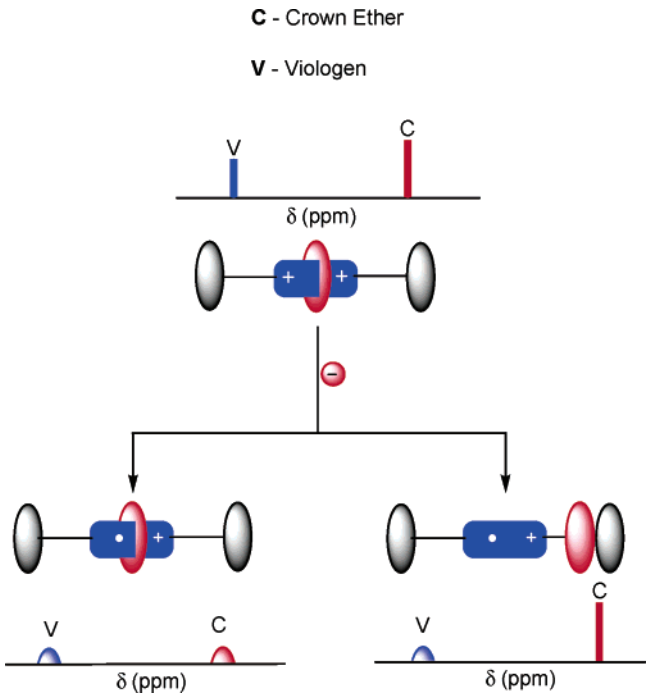

PASSY of Model Axles. Shown in Figure 1 are the ^{1}H NMR spectra of the axle **1**·2PF_6 and the corresponding radical cation **1**$^{\bullet}$·PF_6 formed by a one-electron reduction of the viologen moiety. No resonances are observed for the protons H_1 to H_5 (Scheme 3) of **1**$^{\bullet}$·PF_6 between 0 and 10 ppm.[25] It was concluded that the above resonances are suppressed by PRE in the presence of the unpaired electron localized on the viologen. The corresponding paramagnetic suppression zone (PSZ) is represented in Scheme 3 by a blue ellipsoid and encloses all of the protons of **1**·2PF_6.

In a saturation-recovery experiment, the spin−lattice relaxation times T_1 of the protons H_1 to H_5 of the axle **1**·2PF_6 were measured (Table 1). It was not possible to measure the T_1 relaxation times of the same protons in the corresponding radical cation **1**$^{\bullet}$·PF_6, as these relaxation times were less than 10^{-5} s (Table 1). Clearly the suppression of the resonances assigned to protons H_1 to H_5 in the NMR spectrum of **1**$^{\bullet}$·PF_6 is caused by a dramatic shortening of relaxation times due to the close proximity of the unpaired electron and the associated PRE.

To determine the extent of the PSZ associated with the unpaired electron localized on a viologen incorporated in an axle, we studied the axle **2**·2PF_6 and corresponding radical cation **2**$^{\bullet}$·PF_6 shown in Scheme 3. This axle is similar to **1**·2PF_6 but is longer. It was found that the resonances assigned to the protons H_1 to H_5 are suppressed in **2**$^{\bullet}$·PF_6. Also, it was found that the resonances assigned to protons H_6 to H_9 of **2**$^{\bullet}$·PF_6, although broadened, are not suppressed. On this basis, it was concluded that the PSZ of **2**$^{\bullet}$·PF_6 extends to the benzyl moieties linked to the viologen moiety. The corresponding PSZ is represented in Scheme 3 by a blue ellipsoid.

Because the resonances assigned to the protons H_6 to H_9 are merely broadened, it was possible to measure T_1 relaxation times for these protons in both the axle **2**·2PF_6 and the corresponding

(25) No resonances were observed between −500 and +500 ppm.

Scheme 3. Viologens **1**·2PF_6 to **3**·2PF_6 and the Paramagnetic Suppression Zones of the Corresponding Radical Cations

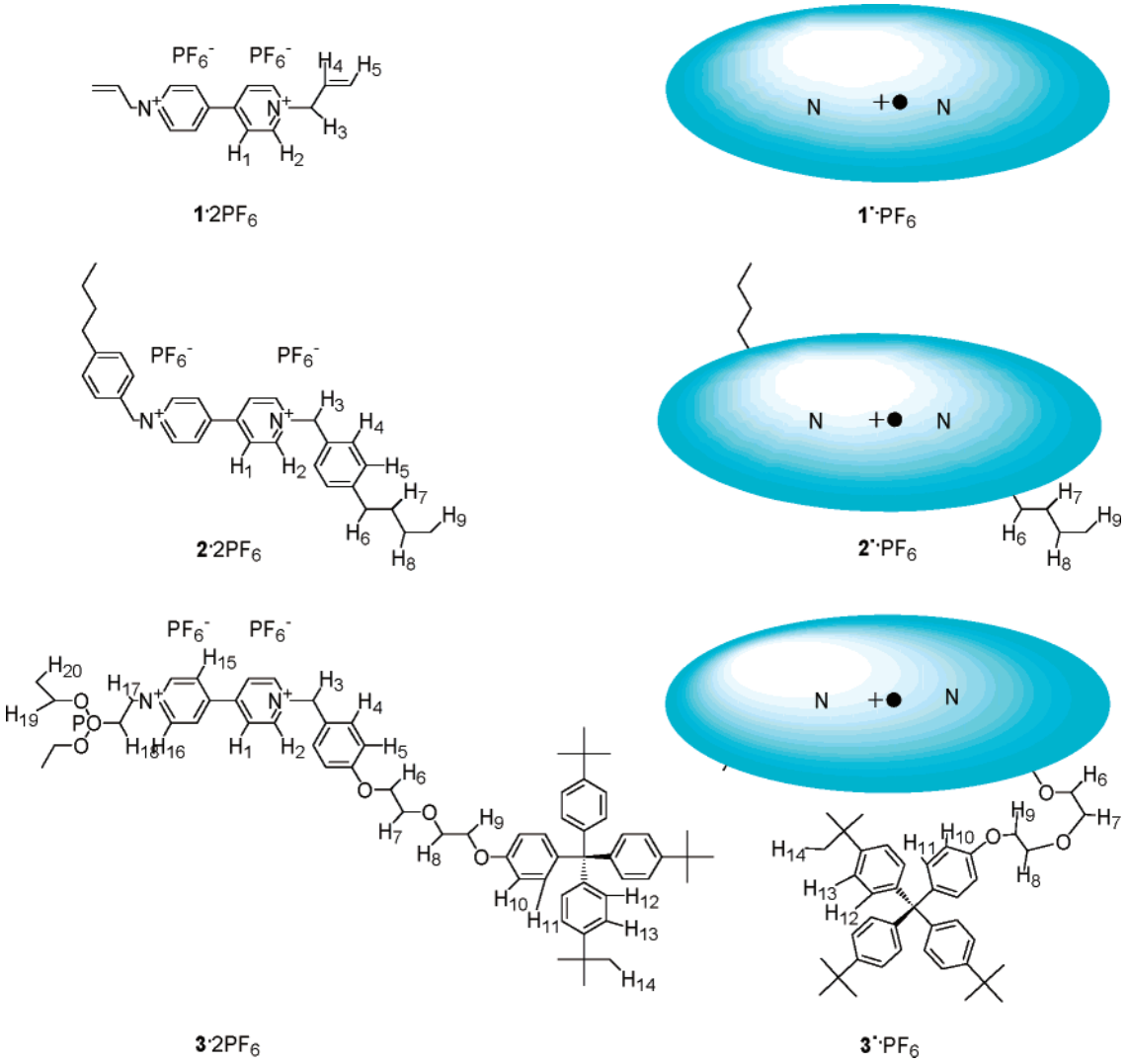

radical cation **2**•·PF_6 (Table 2). Accordingly, it was possible to determine the rate constant for paramagnetic relaxation R_1^e (Table 2). Significantly R_1^e decreases from H_6 to H_9, consistent with an increased separation from the paramagnetic viologen moiety. On this basis, it is concluded that butyl chains of **2**•·PF_6 are, on average, not folded in acetonitrile at 25 °C.

To demonstrate that PASSY can be used to determine the structural conformation in solution of more complex axles, such as those incorporating linker and stopper groups, we studied the axle **3**·2PF_6 and the corresponding radical cation **3**•·PF_6 shown in Scheme 3. It was found that the resonances assigned to the protons of the viologen moiety (H_1, H_2, H_{15}, H_{16}), the adjacent benzyl moiety (H_3 to H_5) and linker group (H_{17} to H_{20}) are suppressed in **3**•·PF_6. Also it was found that the resonances assigned to the protons of the chain linking the viologen moiety and the stopper group (H_6 to H_9) and the stopper group itself (H_{10} to H_{14}) of **3**•·PF_6, although broadened, are not suppressed. On this basis, it was concluded that the PSZ of **3**•·PF_6 extends in one direction to the benzyl moiety linked to the viologen moiety, and in the other direction to the linker group also linked to the viologen moiety. The corresponding PSZ is represented in Scheme 3 by a blue ellipsoid.

Because the resonances assigned to the protons H_6 to H_{14} are merely broadened, it was possible to measure T_1 relaxation times for these protons in both the axle **3**·2PF_6 and the corresponding radical cation **3**•·PF_6 (Table 3). Consequently, it was possible to determine the rate constant for paramagnetic relaxation R_1^e (Table 3). Significantly, R_1^e decreases from H_6 to H_7 and increases from H_8 to H_9. Equally significantly, the values for R_1^e for H_{10} to H_{14} are similar to those for H_7 and H_8. On this basis, it is concluded that the flexible chain linking the viologen moiety and the stopper group is, on average, folded back on itself in **3**•·PF_6 in acetonitrile at 25 °C.

It should be noted that the ESR spectrum of the radical cation of **3**•·PF_6 shows no evidence of dimerization. This finding is consistent with the above conclusion that this axle is folded in solution and that dimerization is precluded. It should also be noted that the ESR spectrum of the radical cation **1**•·PF_6 demonstrates the presence of two different paramagnetic species, one of which is probably the dimer $(\mathbf{1}^{\bullet})^2$·2PF_6. This finding is consistent with the above conclusion that this axle is not folded in solution and that dimerization is not precluded.[26,27]

(26) Evans, A.; Evans, J.; Baker, M. *J. Chem. Soc., Perkin 2* **1977**, 1787−1789;

Scheme 4. [2]Pseudorotaxane **1·5**·2PF_6 and the Paramagnetic Suppression Zone of the Corresponding Radical Cation

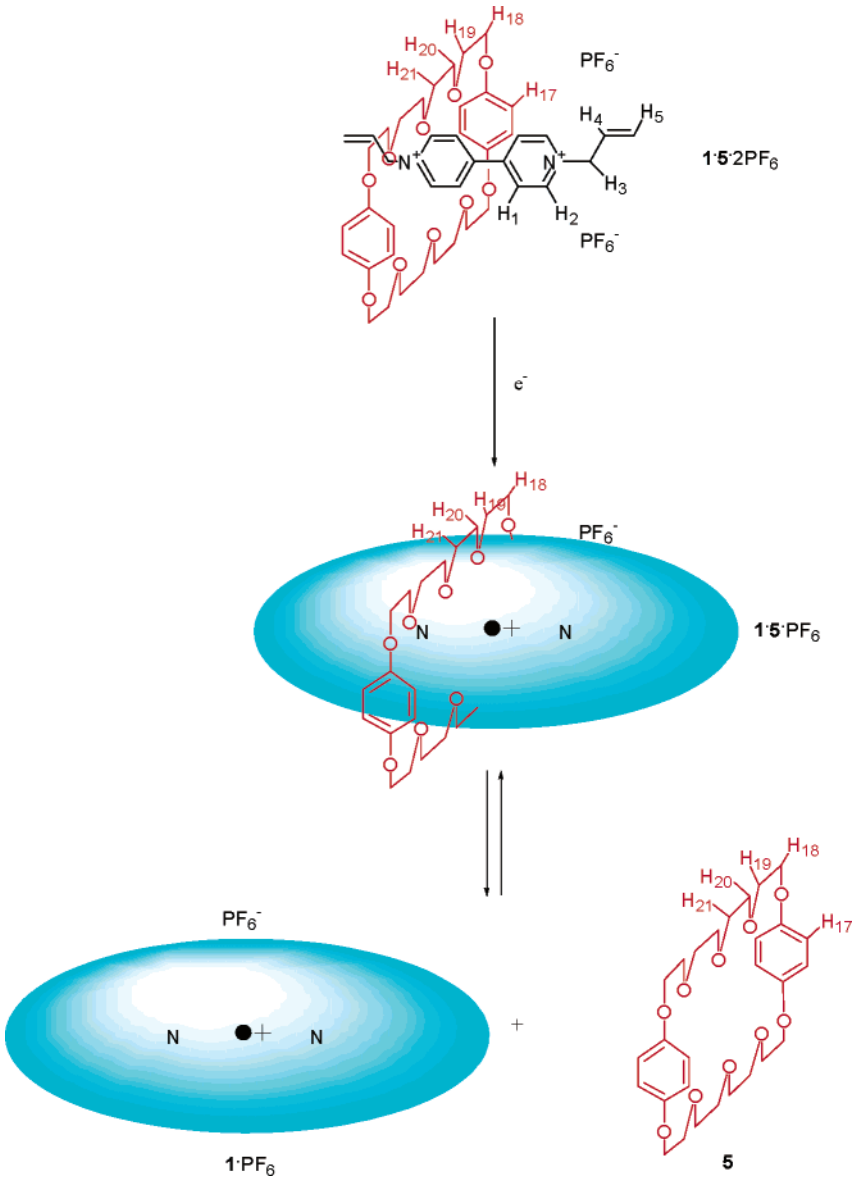

PASSY of Model [2]Pseudorotaxane. In studying the [2]pseudorotaxane **1·5**·2PF_6 (Scheme 4), the objectives were to determine if the crown ether **5** remains complexed with the radical cation formed by a one-electron reduction.

In the presence of the crown ether **5,** the axle **1**·2PF_6 forms the [2]pseudorotaxane **1·5**·2PF_6 shown in Scheme 4. Support for this assertion is provided by the proton NMR spectrum of **1·5**·2PF_6 shown in Figure 1. This spectrum exhibits characteristic upfield shifts of the resonances assigned to the viologen moiety incorporating the axle **1**·2PF_6 and the crown ether **5**. As threading−unthreading is fast on the NMR time scale, the observed chemical shifts are population weighted averages of the chemical shifts for the complexed and uncomplexed axle **1**·2PF_6 and crown ether **5**. It was established spectroscopically that about 30% of the above axles have threaded a crown ether to form the [2]pseudorotaxane.[28]

Following a one-electron reduction of the [2]pseudorotaxane **1·5**·2PF_6, the proton NMR spectrum of the corresponding radical cation **1**$^{\bullet}$**·5**·PF_6 is found to consist only of resonances that can be assigned to the crown ether **5** (Figure 1). Significantly, these resonances are shifted downfield and suggest that 95% of the crown ether **5** is free in solution. Furthermore, these resonances are only slightly broadened. A comparison of the spin−lattice relaxation times T_1 for the crown ether **5** in the [2]pseudorotaxane **1·5**·2PF_6 and in the corresponding radical cation **1**$^{\bullet}$**·5**·PF_6 confirm that the PRE is small (Table 1). The corresponding rate constants for paramagnetic relaxation R_1^e were determined for each of the protons of the crown ether (Table 1). The values determined for R_1^e are consistent with 95% of the crown ether **5** being free in solution. In short, these findings allow us to conclude that reduction of the [2]pseudorotaxane **1·5**·2PF_6 results in essentially complete dissociation of the radical cation of the axle **1**·2PF_6 and the crown ether **5**.

PASSY of Model [2]Rotaxane. In studying the [2]rotaxane **4·5**·2PF_6 (Scheme 5), the objectives were to determine if the crown ether **5** remains localized at the radical cation **4**$^{\bullet}$**·5**·PF_6 formed by a one-electron reduction of the viologen moiety, and

(27) Ivanov, V.; Grishina, A.; Shapiro, B. *Izv. Acad. Nauk SSSR, Ser. Khim.* **1976**, 1383.
(28) Determination of equilibrium constant was as described in ref 10.

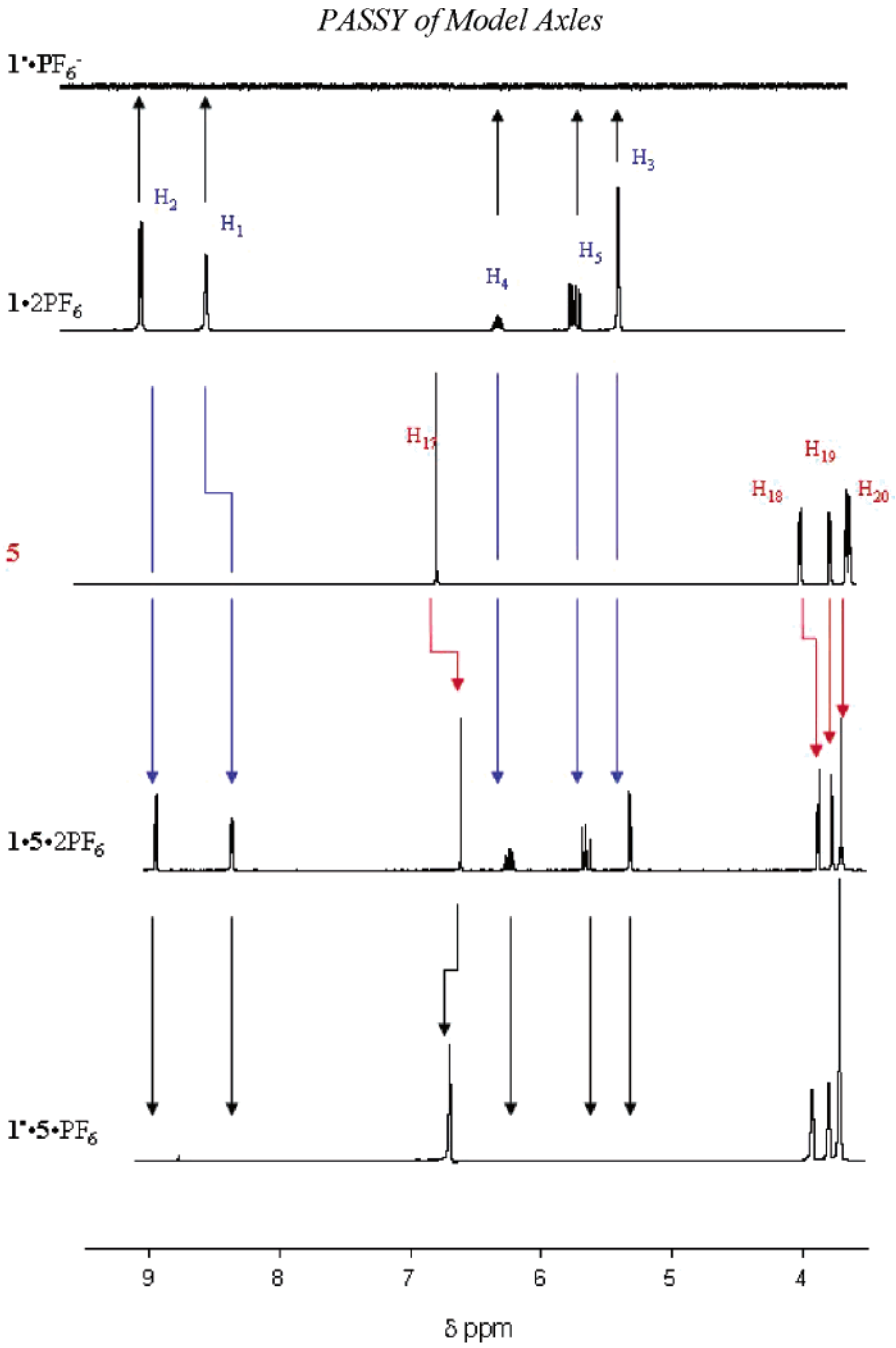

Figure 1. ^{1}H NMR of the axle **1**·2PF$_6$, its radical cation **1**$^{\bullet}$·PF$_6$, the crown ether **5**, the [2]pseudorotaxane **1**·**5**·2PF$_6$ and its radical cation **1**$^{\bullet}$·**5**·2PF$_6$, all in acetonitrile-d_3 at 25° C and 10^{-2} mol dm^{-3}.

if it does, to what extent is this a consequence of the structural conformation of **4**·**5**·2PF$_6$ in solution.

An equimolar mixture of the axle **4**·2PF$_6$ and the crown ether **5**, denoted **4**·2PF$_6$+**5**, and the [2]rotaxane **4**·**5**·2PF$_6$ were studied prior to and following one-electron reduction of the viologen moiety incorporated in the axle **4**·2PF$_6$. The corresponding proton NMR spectra are shown in Figure 2. The measured relaxation times and derived values for R_1^e are given in Table 4.

As expected, no NMR evidence was found for the interaction of the axle **4**·2PF$_6$ and the crown ether **5** in the equimolar mixture **4**·2PF$_6$+**5** (Figure 2 and Table 4). However, characteristic upfield shifts were observed for the resonances assigned to the aromatic protons of the viologen moiety of **4**·2PF$_6$ (H$_1$ and H$_2$) and of **5** (H$_{17}$ to H$_{21}$) in the [2]rotaxane **4**·**5**·2PF$_6$ (Scheme 5). On this basis it was concluded that the crown ether **5** is localized at the viologen moiety of **4**·2PF$_6$ in **4**·**5**·2PF$_6$.[11,16]

Following a one-electron reduction of the axle **4**·2PF$_6$, the resonances assigned to the protons of the viologen moiety and the adjacent benzyl groups of the corresponding radical cation **4**$^{\bullet}$·PF$_6$ are no longer observed for the equimolar mixture of **4**·2PF$_6$ and the crown ether **5**, **4**·2PF$_6$+**5**, or for the [2]rotaxane **4**·**5**·2PF$_6$ (Figure 2). However, the resonances assigned to the crown ether **5**, unchanged for **4**$^{\bullet}$·PF$_6$+**5**, are significantly broadened but shifted only slightly downfield in the radical cation **4**$^{\bullet}$·**5**·PF$_6$ (Figure 2). On this basis, it is concluded that

Table 1. Relaxation Times and Rates in **1**·2PF$_6$ and **1**$^{\bullet}$·**5**·2PF$_6$[a]

assignment	notation	T_1 in **1**·2PF$_6$ (s)	T_1 in **5** (s)	T_1 in **1**·**5**·2PF$_6$ (s)	T_1 in **1**$^{\bullet}$·**5**·PF$_6$ (s)[b]	R_1[e] (s^{-1})
2-pyridinium	2	3.48	–	2.17	$<10^{-5}$	–
3-pyridinium	1	3.62	–	2.17	$<10^{-5}$	–
allyl CH_2	3	1.88	–	1.30	$<10^{-5}$	–
allyl CH=	4	6.52	–	3.91	$<10^{-5}$	–
allyl CH_2=	5	5.07	–	2.75	$<10^{-5}$	–
crown aromatic H	17	–	2.46	1.45	0.29	2.76
crown-α-CH_2	18	–	1.00	0.72	0.26	2.45
crown-β-CH_2	19	–	1.00	0.72	0.43	0.92
crown-γ-CH_2	20	–	1.00	0.72	0.43	0.92
δ-CH_2	21	–	1.00	0.72	0.43	0.92

[a] Acetonitrile, 10^{-2} mol dm^{-3} and 25 °C. [b] T_1 $<10^{-5}$ s cannot be measured.

Table 2. Relaxation Times and Rates in **2**·2PF$_6$[a]

assignment	notation	shift δ (ppm)	T_1 in **2**·2PF$_6$ (s)	T_1 in **2**$^{\bullet}$·PF$_6$[b] (s)	R_1[e] (s^{-1})
2-pyridinium	2	9.00	1.88	$<10^{-5}$	-
3-pyridinium	1	8.39	1.88	$<10^{-5}$	-
benzyl CH_2	3	5.82	0.87	$<10^{-5}$	-
benzyl aromatic	4	7.46	2.61	$<10^{-5}$	-
benzyl aromatic	5	7.39	2.61	$<10^{-5}$	-
chain α-CH_2	6	2.70	1.59	0.22	3.97
chain β-CH_2	7	1.65	1.74	0.26	3.26
chain γ-CH_2	8	1.4	2.03	0.43	1.81
chain δ-CH_2	9	0.98	2.32	0.87	0.72

[a] Acetonitrile, 10^{-2} mol dm^{-3} and 25 °C. [b] T_1 < 10^{-5} s cannot be measured.

Table 3. Relaxation Times and Rates in **3**·2PF$_6$[a]

assignment	notation	shift δ (ppm)	T_1 in **3**·2PF$_6$ (s)	T_1 in **3**$^{\bullet}$·PF$_6$[b] (s)	R_1[e] (s^{-1})
2-pyridinium	2	8.98	1.59	$<10^{-5}$	–
	16	9.01	1.30	$<10^{-5}$	–
3-pyridinium	1	8.43	1.67	$<10^{-5}$	–
	15	8.40	1.67	$<10^{-5}$	–
benzyl CH_2	3	5.80	0.58	$<10^{-5}$	–
benzyl aromatic	4	7.51	1.74	$<10^{-5}$	–
benzyl aromatic	5	7.10	1.45	$<10^{-5}$	–
stopper chain CH_2	6	4.21	0.65	0.22	3.07
	7,8	3.9	0.65	0.36	1.23
	9	4.15	0.65	0.22	3.07
stopper aryloxy	10	6.80	1.16	0.29	2.59
stopper aryloxy	11	7.20	1.16	0.32	2.27
stopper three aryls	12	7.21	1.30	0.32	2.37
stopper three aryls	13	7.37	1.45	0.32	2.45
stopper t-Bu	14	1.34	0.87	0.36	1.61
phosphonoethyl, position 1	17	4.90	0.72	$<10^{-5}$	–
phosphonoethyl, position 2	18	2.60	0.72	$<10^{-5}$	–
ethoxy CH_2O	19	4.1	3.33	$<10^{-5}$	–
ethoxy CH_3	20	1.30	3.33	$<10^{-5}$	–

[a] Acetonitrile, 10^{-2} mol dm^{-3} and 25 °C. [b] T_1 < 10^{-5} s cannot be measured

the crown ether **5** is localized at the viologen incorporated in the axle in the [2]rotaxane **4**·**5**·2PF$_6$, both prior to and following reduction of the viologen.

The rate constants for the paramagnetic relaxation of the crown ether **5** in an equimolar mixture of the axle **4**·2PF$_6$ and the crown ether **5**, denoted **4**·2PF$_6$+**5**, are very small (similar to those measured for **5** in **1**$^{\bullet}$·**5**·PF$_6$), consistent with the fact that the stoppered axle **4**·2PF$_6$ or the corresponding radical cation **4**$^{\bullet}$·PF$_6$ cannot thread the crown ether **5**. By comparison the rate constants for the paramagnetic relaxation of **5** in the radical cation of the [2]rotaxane **4**$^{\bullet}$·**5**·PF$_6$ are very large, consistent with the fact that the crown ether **5** is localized at the viologen moiety incorporated in the stoppered axle **4**·2PF$_6$ or the corresponding radical cation **4**$^{\bullet}$·PF$_6$.

A question that arises is why the crown ether **5** is not delocalized and free to move along the axle **4**$^{\bullet}$·PF$_6$ of the radical cation of the [2]rotaxane **4**$^{\bullet}$·**5**·PF$_6$. The rate constants for paramagnetic relaxation of the protons of the flexible chains linking the stopper groups to the viologen moiety (H_6–H_9) and the protons of the stopper groups (H_{10}–H_{13}) provide the required insight. Specifically, these rate constants are consistent with the flexible chain linking the stopper group being folded back on itself and, as a consequence, with the stopper group being close to the viologen moiety. A possible structural configuration for the [2]rotaxane **4**·**5**·2PF$_6$ in acetonitrile at 25 °C is shown in Scheme 5. It is clear that the above structural conformation precludes shuttling of the crown ether. We are currently undertaking detailed theoretical studies to understand the intramolecular interactions that provide the driving force for the above conformational change. One possibility is that there is a CH-π interaction between the aromatic moieties of the crown ether and the stopper group.

Conclusions

Described is a new NMR technique, namely paramagnetic suppression spectroscopy (PASSY), that has been used to determine the effect of a one-electron reduction on the structural conformation of a model [2]pseudorotaxane and [2]rotaxane in solution.

In summary, it has been shown that a one electron reduction of the [2]pseudorotaxane **1**·**5**·2PF$_6$ leads to dissociation of the axle **1**·2PF$_6$ and the crown ether **5**. It has also been shown that a one electron reduction of the [2]rotaxane **4**·**5**·2PF$_6$ does not lead to the delocalization of the crown ether **5**, which remains at the reduced viologen incorporated in the axle **4**$^{\bullet}$·PF$_6$. This is accounted for by the fact that the axle of the **4**·**5**·2PF$_6$ adopts a folded conformation in solution and hinders translational motion of the crown.

It is expected that this technique will meet in part the need for detailed information about the structural conformation in solution and at surfaces of the growing number of redox-active rotaxanes and catenanes being incorporated into nanoscale devices especially in light of the growing awareness of the dependence of the electromechanical function of these devices on the structural conformation in situ of the incorporated rotaxane or catenane.

Finally, this technique could potentially be applied to a wide range of structure–function problems in chemistry and biochemistry by incorporating a suitable redox label into a molecule or biomolecule.

Experimental Section

Reagents and solvents were purchased from Aldrich Co. and were used as received. All reactions were performed under nitrogen using glassware that was flame dried. Chromatographic separations were performed using silica (Merck, 40–63 μ) in the specified solvent system. Melting points were estimated using a Gallenkamp melting point device and were not corrected.

NMR spectra were recorded using a Varian Inova 300 or a Varian Inova 500 spectrometer in acetonitrile at 25 °C. For the PASSY measurements, solutions (10^{-2} mol dm^{-3}) were initially deoxygenated in the NMR tube (Wilmad 535 PP-8 equipped with a rubber septum

Scheme 5. [2]Rotaxane **4·5**·2PF_6 and the Paramagnetic Suppression Zone of the Corresponding Radical Cation

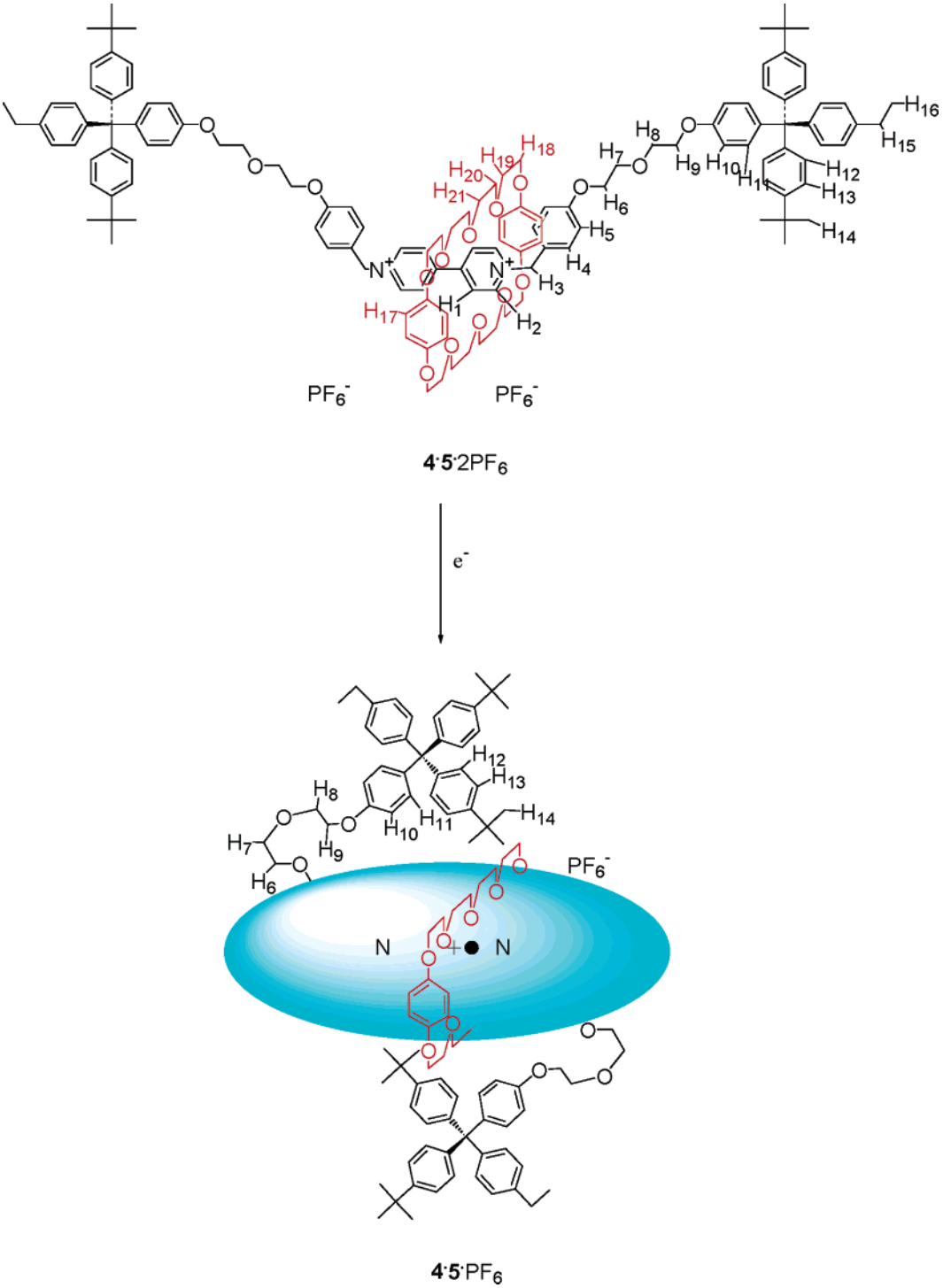

Z124338) by two successive freeze−pump−thaw cycles. Zinc filings (10 mg) were then added and the solutions deoxygenated by further two successive freeze−pump−thaw cycles. Finally the above samples were sonicated for 5 min under nitrogen. NMR spectra of deeply colored solutions of the radical cation were recorded.

T_1 relaxation times were measured using the inversion recovery method on a Varian Inova 500 machine at 25 °C.[29,30] The samples were irradiated using the following: sequence $D_1 = 8$ s and $P_1 = 180°$, D_2 in the range 10^{-5}−2 s and $P_2 = 90°$.

ESR spectra were recorded using a Bruker EMX ESR spectrometer operating with a modulation amplitude of 0.1 G and modulation frequency of 100 kHz at 25 °C. The solutions (10^{-3} mol dm^{-3}) in a chloroform−methanol mixture (9:1 v:v) were placed in ESR tubes and bubbled with nitrogen for 10 min, after which Zn metal dust (10 mg, 200 mesh) was added under continuous flow of nitrogen, and the tubes were sealed again using rubber septa. Measurements were performed after 10 min on the deeply colored solutions.

Mass spectra were run on a Micromass LCT spectrometer.

All compounds were prepared as described below.

1·2PF_6: 1,1′-Diallyl- 4,4′-bipyridinium Bis(hexafluorophosphate. Allyl bromide (0.48 g, 4 mmol) and 4,4′-bipyridyl (0.060 g, 0.40 mmol)

(29) Vold, R. S.; Waught, J. S.; Klein, M. P.; Phelps, D. E. *J. Chem. Phys.* **1968**, *48*, 3831−3832.
(30) Likhtenshtein, G. I.; Adin, I.; Novoselsky, A.; Shames, A.; Vaisbuch, I.; Glaser, R. *Biophys. J.* **1999**, *77*, 443−453.

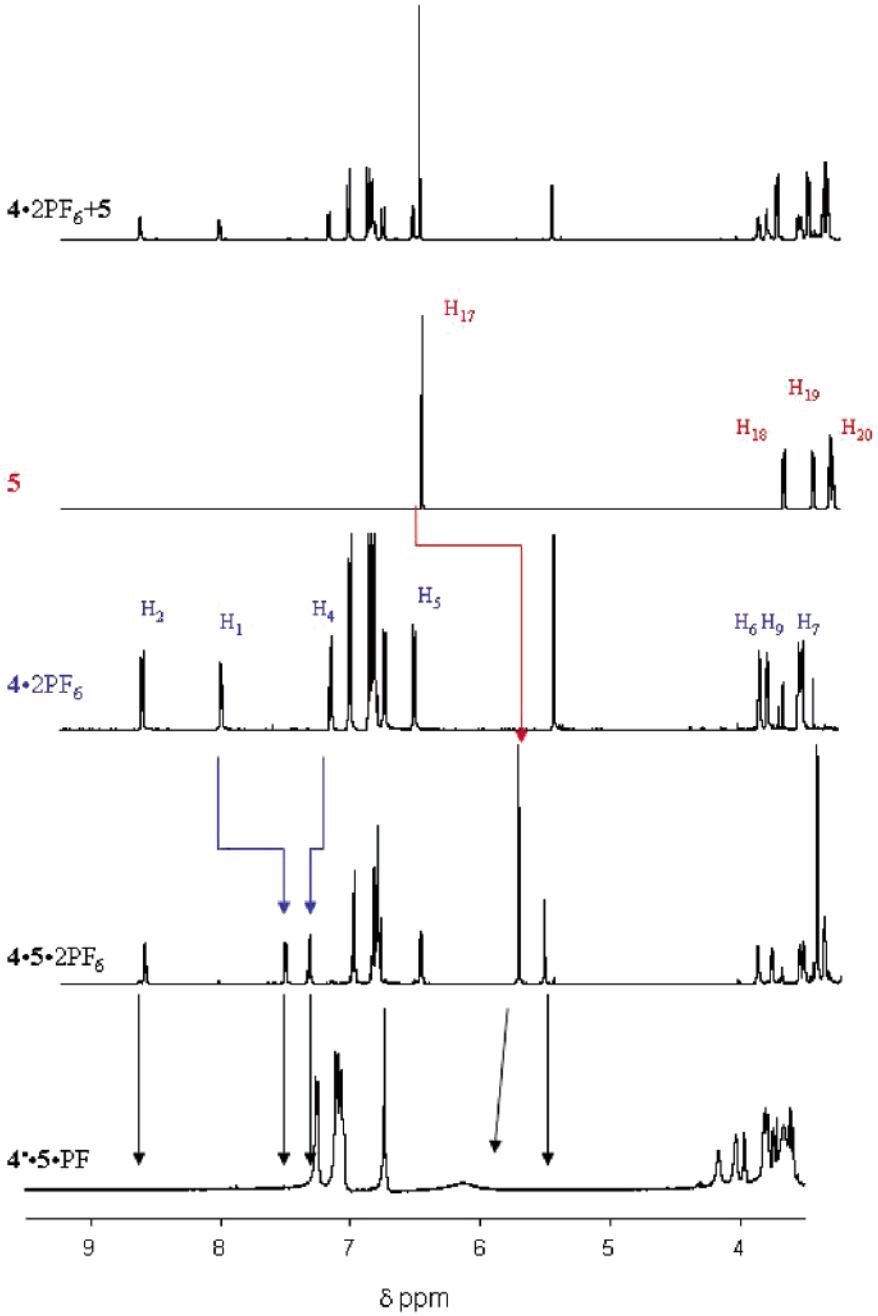

Figure 2. ^{1}H NMR of the axle **4**·2PF$_6$, the crown ether **5**, an equimolar mixture of **4**·2PF$_6$ and **5** denoted **4**·2PF$_6$+**5**, the [2]rotaxane **4·5**·2PF$_6$ and its radical cation **4**•**·5**·2PF$_6$, all in acetonitrile-d_3 at 25 °C and 10^{-2} mol dm^{-3}.

were heated in acetonitrile (10 mL) at 80 °C in a sealed tube for 4 h. The product **1**·2Br (0.145 g, 91%) was dissolved in water (10 mL), and an aliquot of saturated aqueous potassium hexafluorophosphate solution (1 mL) was added to precipitate the insoluble product **1**·2PF$_6$ as a white solid: mp 220 °C (decomposition); ^{1}H NMR (CD$_3$CN) δ 8.90 (d, 4H, J = 7 Hz), 8.40 (d, 4H, J = 7 Hz), 6.16 (m, 2H), 5.6 (m, 4H), 5.24 (d, 4 H, J = 6 Hz); ^{31}P NMR (CD$_3$CN) δ −143 (heptet, J = 712 Hz); Anal. Calcd for $C_{16}H_{18}F_{12}N_2P_2$: C, 36.38; H, 3.43; N, 5.30; Found: C, 35.99; H, 3.25; N, 5.07.

2·2PF$_6$: 1,1′-Bis(4-butylbenzyl)- 4,4′-bipyridinium Bis(hexafluorophosphate). *p*-Butylbenzylbromide (0.171 g, 0.75 mmol) and 4,4′-bipyridyl (0.038 g, 0.25 mmol) were heated in acetonitrile (10 mL) at 80 °C in a sealed tube for 20 h. The product **2**·2Br (0.130 g, 88%) was dissolved in water (10 mL), and an aliquot of saturated aqueous potassium hexafluorophosphate solution (1 mL) was added to precipitate the insoluble **2**·2PF$_6$ as a white solid: mp 240 °C; ^{1}H NMR (CD$_3$CN) δ 9.00 (d, 4H, J = 7 Hz), 8.39 (d, 4H, J = 7 Hz), 7.46 (d, 4H, J = 8 Hz), 7.39 (d, 4H, J = 8 Hz), 5.82 (s, 4H), 2.70 (t, 4H, J = 8 Hz), 1.65 (m, 4H), 1.4 (m, 4H), 0.98 (t, 6H, J = 7 Hz); ^{31}P NMR (CD$_3$CN) δ −151 (heptet, J = 712 Hz); Anal. Calcd for $C_{32}H_{38}F_{12}N_2P_2$: C, 51.90; H, 5.17; N, 3.78. Found: C, 50.95; H, 5.20; N, 3.77.

3·2PF$_6$: 1-[Tris{4-*tert*-butylphenyl}methyl]phenoxyethoxyethoxyphenylmethyl-1′-diethoxyphosphonoethyl-4,4′-bipyridinium Bis(hexafluorophosphate). 1-Diethylphosphonoethyl-4,4′-bipyridinium bromide (35 mg, 0.1 mmol) prepared as described in details elsewhere[31] and 4-[2-[2-[4-tris{4-*tert*-butylphenyl}methylphenoxy]ethoxy]ethoxybenzylbromide (85 mg, 0.11 mmol), also prepared as described in details elsewhere,[9] were heated in toluene (1 mL) and acetonitrile (4 mL) at 80 °C in a sealed tube for 10 h. The dibromide **3**·2Br (95 mg, 80%) was recovered by filtration as a yellow solid: mp 220−230 °C

(31) Rao, S. N.; Fitzmaurice, D. *Helv. Chim. Acta* **1998**, *81*, 902−915.

Table 4. Relaxation Times and Rates in **4**·2PF_6+**5** and **4·5**·2PF_6[a]

		4·2PF_6 + **5**				**4·5**·2PF_6			
assignment	notation	shift δ (ppm)	T_1 in **4**·2PF_6 (s)	T_1 in **4**•·PF_6[b] (s)	R_1[e] (s^{-1})	shift δ (ppm)	T_1 in **4·5**·2PF_6 (s)	T_1 in **4**•·**5**·PF_6[b] (s)	R_1[e] (s^{-1})
2-pyridinium	2	8.86	1.74	$<10^{-5}$	-	8.86	0.87	$<10^{-5}$	-
3-pyridinium	1	8.25	1.74	$<10^{-5}$	-	7.78	0.87	$<10^{-5}$	-
benzyl CH_2	3	5.69	0.58	$<10^{-5}$	-	5.78	0.36	$<10^{-5}$	-
benzyl aromatic	4	7.40	1.59	$<10^{-5}$	-	7.59	1.52	$<10^{-5}$	-
benzyl aromatic	5	6.99	1.45	$<10^{-5}$	-	7.1	1.45	$<10^{-5}$	-
stopper chain CH_2	6	4.10	0.65	0.14	5.37	4.14	0.51	0.07	12.32
	7	3.8	0.58	0.22	2.88	3.8	0.65	0.14	5.60
	8	3.8	0.72	0.22	3.22	3.8	0.65	0.14	5.60
	9	4.04	0.72	0.22	3.22	4.03	0.51	0.17	3.92
stopper aryloxy	10	7.1	1.23	0.17	4.94	7.1	1.30	0.14	6.37
stopper alryloxy	11	6.76	1.45	0.17	5.06	6.73	1.23	0.14	6.33
stopper aryls	12	7.1	1.30	0.12	7.86	7.1	1.30	0.17	5.11
stopper aryls	13	7.26	1.30	0.12	7.86	7.25	1.52	0.17	5.22
stopper t-Bu	14	1.24	1.09	0.22	3.68	1.25	1.09	0.22	3.63
stopper ethyl CH_2	15	2.55	1.12	0.14	6.00	2.56	1.74	0.17	5.31
stopper ethyl CH_3	16	1.14	1.88	0.22	4.07	1.16	2.17	0.22	4.08
crown aromatic H	17	6.74	1.74	1.01	0.41	5.98	1.12	0.0043	231.6
crown α-CH_2	18	3.99	0.80	0.65	0.28	3.7	0.43	0.014	69.1
crown β-CH_2	19	3.75	0.80	0.80	0.00	3.7	0.43	0.014	69.1
crown γ-CH_2	20	3.6	0.80	0.80	0.00	3.6	0.39	0.014	68.8
crown δ-CH_2	21	3.6	0.80	0.80	0.00	3.5	0.39	0.014	68.8

[a] Acetonitrile, 10^{-2} mol dm^{-3} and 25 °C. [b] $T_1 < 10^{-5}$ s cannot be measured.

(decomposition). Anal. Calcd for $C_{64}H_{79}Br_2N_2O_6P$: C, 66.09; H, 6.85; N 2.41; Br. 13.74. Found: C, 65.88; H, 6.50; N, 2.11; Br, 13.20.

3·2Br was dissolved in water (5 mL) treated with saturated potassium hexafluorophospate solution and purified by column chromatography (methanol:nitromethane) yielding **3**·2PF_6 as a yellow solid: mp 218 °C (decomposition); ^{1}H NMR (CD_3CN) δ 9.01 (d, 2H, $J = 6$ Hz), 8.98 (d, 2H, $J = 6$ Hz), 8.43(d, 2H, $J = 6$ Hz), 8.40 (d, 2H, $J = 6$ Hz), 7.51(d, 2H, $J = 8$ Hz) 7.37 (d, 6H, $J = 8$ Hz), 7.21 (d, 6H, $J = 8$ Hz), 7.20 (d, 2H, $J = 8$ Hz), 7.10 (d, 2H, $J = 8$ Hz), 6.8 (d, 2H, $J = 8$ Hz), 5.80 (s, 2H), 4.90 (t, 2H, $J = 7$ Hz), 4.21 (t, 2H, $J = 5$ Hz), 4.15 (t, 2H, $J = 5$ Hz), 4.1(m, 4H), 3.9 (m, 4H), 2.6 (dt, 2H, $J_{HP} = 18$ Hz, $J_{HH} = 7$ Hz), 1.34 (s, 27H), 1.30 (t, 3H, $J = 7$ Hz); ^{31}P NMR δ 18.3 (s), −151 (heptet, $J = 712$ Hz); MS (ES) *m*/*z* 1002 (M+; 22%). Anal. Calcd For $C_{65}H_{83}F_{12}N_2O_6P_3$: C, 59.63; H, 6.39; N, 2.14. Found: C, 59.03; H 6.40; N 2.10.

4·2PF_6: 1,1′-Bis-(4-(2-(2-(4-[bis{4-*tert*-butylphenyl}-4-ethylphenyl-methyl]phenoxy)ethoxy)ethoxy)benzyl)-4,4′-bipyridinium bis-(hexafluorophosphate). This compound was prepared according to the procedure reported.[9]

^{1}H NMR (CD_3CN) δ 8.86 (d, 4H, $J = 7$ Hz), 8.25 (d, 4H, $J = 7$ Hz), 7.40 (d, 4H, $J = 9$ Hz), 7.26 (d, 8H, $J = 9$ Hz), 7.0−7.2 (m, 20 H), 6.99 (d, 4H, $J = 9$ Hz), 6.76 (d, 4H, $J = 9$ Hz), 5.69 (s, 4H), 4.10 (m, 4H), 4.04 (m, 4H), 3.8 (m, 8H), 1.26 (s, 54 H), 2.55 (q, 4H, $J = 7$ Hz), 1.24 (s, 36 H), 1.14 (t, 6H, $J = 7$ Hz).

4·5·2PF_6: 1,1′-Bis-(4-(2-(2-(4-[bis{4-*tert*-butylphenyl}-4-ethylphenyl-methyl]phenoxy)ethoxy)ethoxy)benzyl)-4,4′-bipyridinium Bis-*p*-phenylene-34-crown-10-bis(hexafluorophosphate). This compound was prepared according to the procedure reported.[9]

^{1}H NMR ($CDCl_3$) δ 8.86 (d, 4H, $J = 7$ Hz), 7.78 (d, 4H, $J = 7$ Hz), 7.59 (d, 4H, $J = 9$ Hz), 7.25 (d, 8H, $J = 9$ Hz), 7.1 (m, 24H), 6.73 (d, 4H, $J = 9$ Hz), 5.98 (s, 8H), 5.78 (s, 4H), 4.14 (m, 4H), 4.03 (m, 4H), 3.8 (m, 8H), 3.7 (s, 16H), 3.6 (m, 8H), 3.5 (m, 8H), 2.56 (q, 4H, $J = 7$ Hz), 1.25 (s, 36 H), 1.16 (t, 6H, $J = 7$ Hz).

5: Bis-*p*-phenylene-34-crown-10. This compound was prepared according to the procedure reported.[32]

^{1}H NMR (CD_3CN) δ 6.74 (s, 8H), 3.99 (m, 8H), 3.75 (m, 8H), 3.60−3.64 (m, 16H).

Acknowledgment. This research was supported by Science Foundation Ireland and by Enterprise Ireland. We thank Drs. D. Collison, E. McInnes, and J. Zhao of the EPSRC UK National EPR Service at Manchester. We also thank Dr. K. Glass and Ms. G. Fitzpatrick of the Chemical Services Unit (NMR) at University College Dublin.

JA050694H

(32) Helgeson, R. C.; Tarnowski, T. L.; Timko, J. M.; Cram, D. J. *J. Am. Chem. Soc.* **1977**, *99*, 6411−6419.